Molecular Biology of the Cell
Vol. 11, 3277–3288, October 2000

The Diabetes Autoantigen ICA69 and Its *Caenorhabditis elegans* Homologue, *ric-19*, Are Conserved Regulators of Neuroendocrine Secretion

Marc Pilon,* Xiao-Rong Peng,* Andrew M. Spence,† Ronald H.A. Plasterk,‡ and Hans-Michael Dosch*§

*Departments of Pediatrics and Immunology, University of Toronto, The Hospital for Sick Children, Research Institute, Toronto, Ontario, Canada M5G 1X8; †Department of Molecular and Medical Genetics, University of Toronto, Toronto, Ontario, Canada, M5S 1A8; and ‡Division of Molecular Biology, The Netherlands Cancer Institute, 1066 CX Amsterdam, The Netherlands

Submitted March 6, 2000; Revised June 16, 2000; Accepted July 14, 2000
Monitoring Editor: Judith Kimble

ICA69 is a diabetes autoantigen with no homologue of known function. Given that most diabetes autoantigens are associated with neuroendocrine secretory vesicles, we sought to determine if this is also the case for ICA69 and whether this protein participates in the process of neuroendocrine secretion. Western blot analysis of ICA69 tissue distribution in the mouse revealed a correlation between expression levels and secretory activity, with the highest expression levels in brain, pancreas, and stomach mucosa. Subcellular fractionation of mouse brain revealed that although most of the ICA69 pool is cytosolic and soluble, a subpopulation is membrane-bound and coenriched with synaptic vesicles. We used immunostaining in the HIT insulin-secreting β-cell line to show that ICA69 localizes in a punctate manner distinct from the insulin granules, suggesting an association with the synaptic-like microvesicles found in these cells. To pursue functional studies on ICA69, we chose to use the model organism *Caenorhabditis elegans*, for which a homologue of ICA69 exists. We show that the promoter of the *C. elegans* ICA69 homologue is specifically expressed in all neurons and specialized secretory cells. A deletion mutant was isolated and found to exhibit resistance to the drug aldicarb (an inhibitor of acetylcholinesterase), suggesting defective neurotransmitter secretion in the mutant. On the basis of the aldicarb resistance phenotype, we named the gene *ric-19* (resistance to inhibitors of cholinesterase-19). The resistance to aldicarb was rescued by introducing a *ric-19* transgene into the *ric-19* mutant background. This is the first study aimed at dissecting ICA69 function, and our results are consistent with the interpretation that ICA69/RIC-19 is an evolutionarily conserved cytosolic protein participating in the process of neuroendocrine secretion via association with certain secretory vesicles.

INTRODUCTION

Two main types of specialized secretory vesicles are found in insulin-secreting β-cells: dense-core insulin secretory vesicles, which contain a cargo of semicrystalized insulin granules, and lighter synaptic-like microvesicles (SLMVs), which carry a cargo of neurotransmitters such as γ-aminobutyric acid. Type I diabetes results from the autoimmune destruction of pancreatic β-cells, and most of the known protein targets of the diabetogenic autoimmune attack have in common that they are components of the secretory vesicles found in β-cells. Autoantigens include proinsulin (Palmer *et al.*, 1983), carboxypeptidase H (Castano *et al.*, 1991), glutamate decarboxylase (GAD) (Baekkeskov *et al.*, 1990), 38-kDa protein (Roep *et al.*, 1990), IA-2/ICA512 (Lan *et al.*, 1994; Rabin *et al.*, 1994; Solimena *et al.*, 1996) and its related protein phogrin (Hawkes *et al.*, 1996), the Glima-38 antigen (Aanstoot *et al.*, 1996), and the GM2-1 ganglioside (Dotta *et al.*, 1998). Although diabetes is primarily a β-cell–specific autoimmune disease, expression of the autoantigens is usually not restricted to this cell type but rather exhibits much broader neuroendocrine tissue distribution. For example, GAD, which is found within SLMVs in β-cells (Reetz *et al.*, 1991), has extremely low levels of expression in the islets but exhibits high expression levels in brain, testis, and other neuroendocrine tissues (Faulkner-Jones *et al.*, 1993; Petersen *et al.*, 1993). Similarly, IA-2 is a vesicular integral membrane phosphotyrosine phosphatase–like protein that exhibits a

§ Corresponding author. E-mail address: hmdosch@sickkids.on.ca.

broad neuroendocrine expression pattern and that has been suggested to regulate vesicle trafficking in conjunction with the related protein phogrin (Solimena *et al.*, 1996; Wasmeier and Hutton, 1996; Wishart and Dixon, 1998).

ICA69 (islet cell autoantigen of 69 kDa) is a novel protein that is also a common target of diabetic autoimmunity in humans and diabetes-prone rodents (Pietropaolo *et al.*, 1993; Miyazaki *et al.*, 1994, 1995; Martin *et al.*, 1995; Roep *et al.*, 1996; Karges *et al.*, 1997). The primary sequence of the ICA69 protein provides few clues to its function, although computer analysis suggests that ICA69 is a cytosolic soluble protein remarkably rich in α helices and containing a short coiled-coil motif. The in vivo expression pattern of ICA69 has been controversial (Karges *et al.*, 1996, 1997; Mally *et al.*, 1996; Stassi *et al.*, 1997), presumably because of low expression levels. However, Western blot analysis has consistently detected high levels of ICA69 in brain and pancreas and, among cell lines, the highest levels of ICA69 have been found in pancreatic β-cell lines (Pietropaolo *et al.*, 1993; Karges *et al.*, 1996).

We wished to discover the function of ICA69 and, in particular, to determine whether ICA69 participates in the process of neuroendocrine secretion, as do most of the other diabetes autoantigens. Here we show that ICA69 expression levels among rodent tissues correlate loosely with secretory activity, with the highest levels found in brain, pancreas, and stomach mucosa. Using brain fractionation and immunostaining of a β-cell line, we also present evidence that a subpopulation of ICA69 molecules is associated with secretory vesicles.

To address ICA69 function more directly, we chose to use the model organism *Caenorhabditis elegans*, for which a predicted gene bearing high homology with ICA69 exists. *C. elegans* is a small nematode of which the complete 100-megabase genome sequence is available (*C. elegans* Sequencing Consortium, 1998). *C. elegans* is particularly suitable for genetic and developmental studies because of its short generation time, ease of culture, and small cell number (adult hermaphrodites are composed of 959 cells). Any deviation from normal development can be identified precisely, because *C. elegans* exhibits an essentially invariant cell lineage from egg to adult. Finally, the entire nervous system has been described at the ultrastructural level (White *et al.*, 1986; Wood, 1988; Riddle *et al.*, 1997).

The predicted *C. elegans* gene C32E8.7 encodes a homologue of ICA69 (*C. elegans* Sequencing Consortium, 1998). In the studies reported here, we show that the C32E8.7 promoter is expressed in apparently all *C. elegans* neurons as well as in the excretory canal cell and its associated gland cell. We isolated a C32E8.7 deletion mutant and found that this mutant exhibits resistance to the drug aldicarb, suggesting a defect in neurotransmitter secretion in the mutant. On the basis of this phenotype, we named the gene *ric-19* (resistance to inhibitors of cholinesterase-19) and will refer to it as such in this paper. Our results argue for an evolutionarily conserved function for the ICA69 homologues in secretory cells, and the *ric-19* mutant should prove valuable to further dissect ICA69 function.

MATERIALS AND METHODS

Western Blotting

For the mouse tissue and brain fractionation immunoblots, a rabbit antiserum generated against the C-terminal 12 amino acids of the human ICA69 (a kind gift from M. Pietropaolo, Children's Hospital, Pittsburgh, PA; Pietropaolo *et al.*, 1993) was used at a final dilution of 1:5000. A total of 40 μg of protein from the postnuclear supernatant (fraction S1; see below) of tissues or cells was loaded in each lane, electrophoresed on a SDS polyacrylamide gel, and transferred to nitrocellulose. Blotto (5% skim milk powder in PBS containing 0.1% Tween-20) was used for blocking. Antibody dilutions and washes were carried out in PBS containing 0.1% Tween-20 (Harlow and Lane, 1988). A goat anti-rabbit HRP-conjugated secondary antibody (Jackson Laboratories, Bar Harbor, ME) was used at a final concentration of 1:15,000 to detect bound primary antibody.

For *C. elegans* Western blot detection of the RIC-19 protein, the rabbit antiserum 6097 was generated by immunizing a rabbit against a peptide corresponding to the 20 C-terminal amino acids of the predicted RIC-19 protein (Genemed Synthesis, San Francisco, CA). Antibody 6097 was affinity purified with the peptide used for immunization and used at a 1:5000 dilution for Western blots. Crowded plates of various *C. elegans* strains were harvested and washed twice in water before lysis by boiling in SDS sample loading buffer. Five micrograms of total protein was loaded on a SDS polyacrylamide gel and detected as described above.

Subcellular Fractionation of Mouse Brain

Different subcellular fractions of mouse brain were prepared as described (Huttner *et al.*, 1983). Briefly, two mouse brains were homogenized in 5 ml of ice-cold H buffer (0.3 M sucrose, 10 mM HEPES-KOH, pH 7.5, 1 mM EGTA, 0.1 mM EDTA, 0.3 mM PMSF) with the use of a loose-fitting Teflon/glass homogenizer with 10 full strokes. The homogenate was centrifuged at 1000 $\times$ *g* for 10 min to remove nuclei and cell debris, and the supernatant (S1) was transferred to a new tube and centrifuged at 13,000 $\times$ *g* for 13 min. The supernatant was collected and spun at 100,000 $\times$ *g* for 30 min to yield S3 (the cytosol) and P3 (the microsomal pellet). The pellet (P2), which is enriched in synaptosomes, was washed once in HBS buffer (10 mM HEPES-KOH, pH 7.5, 142 mM NaCl, 2.4 mM KCl, 1 mM $MgCl_2$, 5 mM glucose, 0.1 mM EGTA, 0.3 mM PMSF) and centrifuged once more at 13,000 $\times$ *g* for 13 min. The P2 fraction was then lysed in 10 ml of ice-cold H_2O, 0.3 mM PMSF for 30 min, buffered with 1 M HEPES-KOH, pH 7.4, to a final concentration of 10 mM, and centrifuged at 45,000 $\times$ *g* for 20 min. The pellet (LP1) was resuspended in HKA buffer (10 mM HEPES-KOH, pH 7.4, 140 mM potassium acetate, 1 mM $MgCl_2$, 0.1 mM EGTA) in the presence of 0.3 mM PMSF, whereas the crude synaptic vesicles were pelleted by further centrifuging the supernatant at 150,000 $\times$ *g* for 1 h and resuspended in HKA buffer. All procedures were performed at 4°C. Control antibodies used were as follows: a rabbit polyclonal antibody against VAMP-2 was a gift from W. Trimble (Hospital for Sick Children, Toronto, Canada; Gaisano *et al.*, 1994); a mouse monoclonal anti-SUMO-1 antibody was purchased from Zymed (San Francisco, CA; Mahajan *et al.*, 1997); a mouse monoclonal anti-NMDAR antibody was purchased from PharMingen International (San Diego, CA; Siegel *et al.*, 1994); and a mouse monoclonal anti-β-tubulin antibody (Chu and Klymkowsky, 1989) was obtained from the Developmental Studies Hybridoma Bank at the University of Iowa (Ames, Iowa).

Immunostaining of HIT-1 Cells

Hamster insulinoma HIT-1 cells were grown on polylysine-coated coverslips in RPMI-1640 supplemented with 10% FCS. Cells were fixed in 4% paraformaldehyde in PBS for 15 min, quenched with the use of 0.1 M glycine in PBS for 10 min, followed by permeabilization and blocking in 10% normal goat serum, 0.1% gelatin, 0.1% Triton X-100 in PBS for 15 min. The cells were then incubated with primary antibodies diluted in blocking buffer for 1 h at room temperature. After washing three times in PBS containing 0.1% Triton X-100 (10 min for each wash), the cells were incubated with the secondary antibody for 1 h at room temperature and then washed again.

Antibodies used were as follows: guinea pig anti-insulin and guinea pig control antibody were purchased from DAKO Diagnostics Canada Inc. (Mississauga, Ontario, Canada); the peptide antibody against ICA69 was used at a 1:1000 dilution; a polyclonal antibody against SNAP-25 (produced in house against a recombinant protein) was a gift from W. Trimble and used at a 1:250 dilution; donkey anti-guinea pig (TRITC-conjugated) and donkey anti-rabbit (FITC-conjugated) antibodies were purchased from Jackson Laboratories and used at a 1:2500 dilution. The cells were mounted onto glass slides with mounting medium (DAKO) and documented with a fluorescence microscope.

Nematode Strains and Culturing

General methods for the culture, manipulation, and genetics of *C. elegans* were as described (Sulston and Hodgkin, 1988). Unless indicated otherwise, strains were cultured at 20°C. Strains used in this study were the wild-type Bristol N2, obtained from the *Caenorhabditis* Genetics Center (St. Paul, MN); AS241 [*ric-19(pk690)*]; and NW1229, which carries the integrated array *evIs111* (a gift from J. Culotti, University of Toronto, Toronto, Ont., Canada). *evIs111* contains the plasmids pPD#SU006 (expressing green fluorescent protein [GFP] panneurally) and pMH86 (encoding *dpy-20(+)*).

Plasmids

pRIC-19, which contains the entire predicted *ric-19* gene as well as 642 nucleotides of 5′ flanking region and 76 nucleotides of 3′ flanking region, was constructed by subcloning a *Hin*dIII fragment from the cosmid C32E8 (obtained from the Alan Coulson, The Sanger Centre, Hinxton, United Kingdom) into the corresponding site of pBS SK (Stratagene, La Jolla, CA).

In the PCR amplification reactions used for the construction of reporter plasmids, the high-fidelity rTth polymerase (Perkin Elmer-Cetus, Norwalk, CT) was used to amplify the appropriate regions of the C32E8 cosmid. The final plasmids were sequenced over the amplified regions. The primers CelicaP1 (5′-gaactgcagctccgattgtctctacgatcatcc-3′; *Pst*I site underlined) and CelicaP2 (5′-cgctctagagagccgagtcatgaatctatctgc-3′; *Xba*I site underlined) were used to amplify the promoter region and the first 10 codons of the *ric-19* gene (designated C32E8.7 by the *C. elegans* Sequencing Consortium). Amplification yielded a fragment encompassing nucleotides −1068 to +30 of the *ric-19* gene, where +1 indicates the A of the start codon. This fragment was then subcloned as a *Pst*I and *Xba*I insert into the corresponding sites of pPD95.69 and pPD95.57 (A. Fire, personal communication) to produce the reporter constructs pCelicaP-GFP and pCelicaP-*lacZ*, respectively. The plasmid pCelicaDP-GFP is a derivative of pCelicaP-GFP from which a *Hin*dIII fragment has been excised so that only nucleotides −641 to +30 of the *ric-19* gene are retained in frame with the GFP gene.

The pRIC19::GFP plasmid, which encodes a full-length RIC-19 protein–GFP fusion under the control of 1.5 kilobase (kb) of *ric-19* 5′ flanking sequence, was constructed in several steps. First, a 5.16-kb product spanning positions −1547 to +3258 was amplified with the use of the primers CelicaGFP1 (5′-gaactgcaggaatggcatcgatctgaaaggg-3′; *Pst*I site underlined) and CelicaGFP2 (5′-cgctctagacaacaagttatcctcattctctc-3′; *Xba*I site underlined) and then subcloned as a *Pst*I–*Xba*I fragment into the corresponding sites of pBS KS (Stratagene) to generate pC32E8.7*. Second, a 1.85-kb product encompassing the GFP coding sequence and *unc-54* 3′ untranslated region was amplified from the pPD95.69 plasmid with the use of the primers CelicaGFP3 (5′-cgctctagaatgagtaaaggagaagaacttttcac-3′; *Xba*I site underlined) and CelicaGFP4 (5′-gtgaccgcggttacagacaagctgtgaccgtc-3′; *Sac*II site underlined) and then subcloned as a *Xba*I–*Sac*II fragment into the corresponding sites of pC32E8.7* to generate the construct pRIC19::GFP.

Transgenic Animals

C. elegans transformation was carried out with the use of the methods described by Mello and Fire (1995). Hermaphrodites of either strain N2 or AS241 were injected with a DNA mixture containing 50 μg/μl plasmid pRF4, which carries the transformation marker *rol-6(su1006dm)* (Mello *et al.*, 1991), and 50 μg/μl test plasmid. Transgenic lines carrying the injected DNA on extrachromosomal arrays were established from F_2 Rol progeny of injected animals. For rescue experiments, *ric-19* mutant animals (see below) carrying an integrated copy of the pRIC-19 plasmid were generated as follows: transgenic AS241 animals carrying an extrachromosomal array harboring pRIC-19 and the panneuronal GFP reporter pPD#SU006 were first generated as described above. Integration of the array was subsequently induced by γ-ray irradiation (3000 rad) of transgenic L4 larvae. The F_2 progeny of irradiated animals were screened for animals with 100% transmission of the GFP marker over several generations and six back-crosses to AS241 animals. One stable line was obtained.

A ric-19 Deletion Mutant

A deletion mutation of *ric-19* was isolated as described (Jansen *et al.*, 1997). The primers AL1 (5′-cgacgacactccattattcc-3′) and AR1 (5′-ccagtcctgcaaaaatgctc-3′) and nested primers AL2 (5′-tgagggttttcctgtgaagg-3′) and AR2 (5′-gttttgcccaacgattgtct-3′) were used in a PCR screen for *ric-19* deletion mutants among a frozen library of chemically mutagenized *C. elegans*. A 2.6-kb deletion allele, *ric-19(pk690)*, was isolated and the PCR product detecting the deletion was sequenced directly. The deletion was found to span nucleotides −354 to +2276 of the predicted *ric-19* gene. The *pk690* allele was backcrossed 10 times to an N2 background to generate strain AS241.

Phenotypic Characterization

Assays for the following phenotypic traits were as described elsewhere: life span (Kenyon *et al.*, 1993), chemotaxis (Bargmann *et al.*, 1993), self-brood size (Wong *et al.*, 1995), defecation cycle length (Thomas, 1990), defecation expulsion frequency (Thomas, 1990; Miller *et al.*, 1996), thermal tolerance (Anderson, 1978), thrashing rate (Miller *et al.*, 1996), and osmotic avoidance (Culotti and Russell, 1978). To synchronize animals for tests that require age-matched animals (life span, self-brood size, defecation cycle length, and thermal tolerance), adults were allowed to lay eggs during a 2-h period, after which the adults were removed; time zero for the test animals was considered to be the middle of the 2-h egg-laying period. Examination of the neuroarchitecture was achieved through the panneuronal GFP marker in the integrated array *evIs111*; *ric-19* animals carrying this array were generated by crossing AS241 males with NW1229 hermaphrodites and recovering animals homozygous for *ric-19(pk690)* and *evIs111* among the F_2 progeny.

Aldicarb was purchased from ChemService (West Chester, PA), and resistance was determined with the use of two assays. The growth rate/dose-response assay was performed as described elsewhere with the use of triplicate plates (Nonet *et al.*, 1993). In this assay, growth rate is defined as the reciprocal of the generation time, and the relative growth rate is defined as the ratio of the growth rate in the presence of aldicarb to the growth rate in the absence of aldicarb. The generation time was arbitrarily defined as the time required for 200 newly hatched larvae to grow and produce 200 new larvae. For the second assay, ~150 larvae (16 h old) per genotype were deposited onto each of five NGM agar plates (Sulston and Hodgkin, 1988) containing 1 mM aldicarb, the plates were blinded, and the number of worms on each plate was determined every 24 h for 10 d. In this assay, growth was defined as the ratio of the number of animals at a given time to the starting number of animals.

RESULTS

Tissue Distribution of Expression in the Mouse

We sought to determine if the mammalian ICA69 protein exhibits an expression profile consistent with a possible role

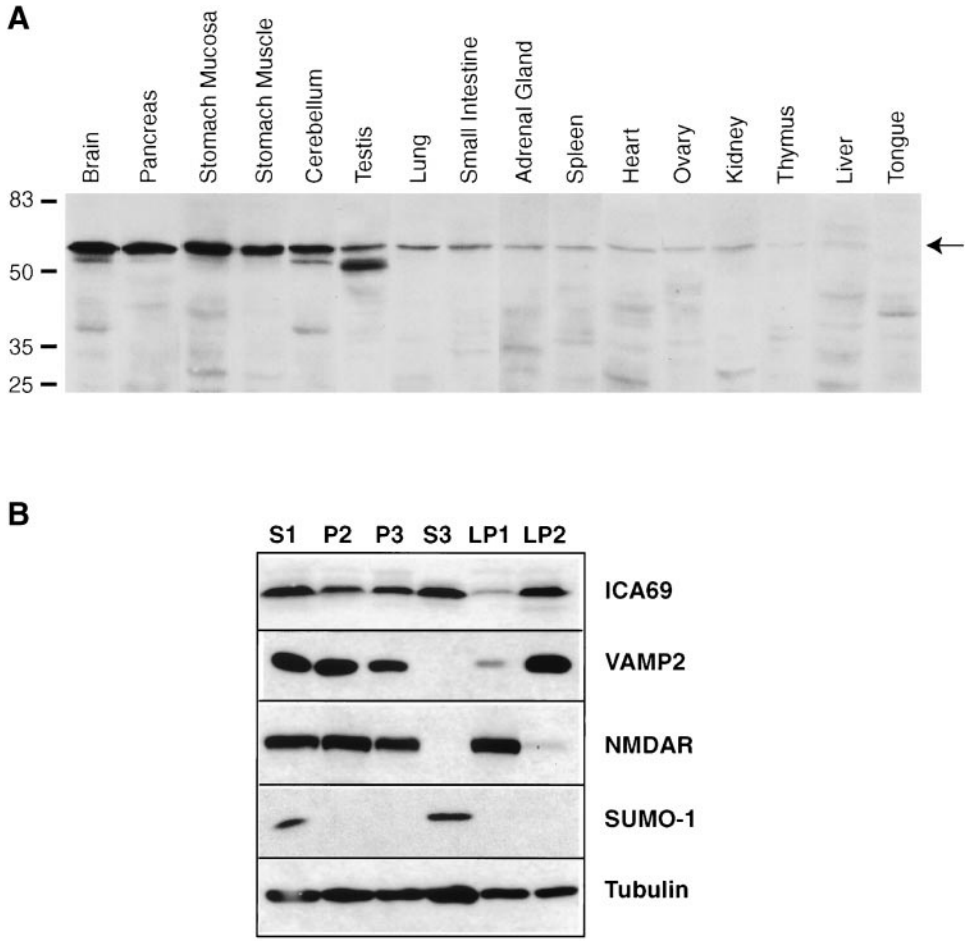

Figure 1. (A) Tissue distribution of mouse ICA69. A total of 40 μg of protein from the various tissues was loaded in each lane. The predominant ICA69 band is indicated by the arrow. (B) Subcellular fractionation of mouse brain and Western blot detection of ICA69, VAMP-2, NMDAR, SUMO-1, and β-tubulin is shown. The nature of the different fractions is as follows: S1, postnuclear supernatant; P2, crude synaptosomes; P3, microsomes; S3, cytosolic soluble; LP1, plasma membranes of synaptosomes; LP2, synaptic vesicles. A total of 40 μg of protein was loaded in each lane.

in secretion. Figure 1A shows the tissue distribution of ICA69 expression in the mouse. The expression levels loosely correlate with the secretory activity of the various tissues. In particular, we observed the highest expression in brain, pancreas, and stomach mucosa, which are tissues specialized in regulated secretory activities. Also, stomach muscle is rich in autonomic fibers, and testis is an important neuroendocrine tissue. The correlation between ICA69 expression levels and secretory activity is not strict, however; in particular, the adrenal gland and the ovary expressed relatively low levels of ICA69. We also observed that the ICA69 band appears as a doublet in some tissues (brain, cerebellum, pancreas, and testis), suggesting that ICA69 may be present in differently processed or modified forms.

Subcellular Fractionation of Mouse Brain

The possible association of ICA69 with secretory vesicles was investigated by subcellular fractionation of brain tissue (Figure 1B). Although most of the ICA69 protein was found within the cytosolic soluble fraction (S3), we found that a significant fraction of the ICA69 protein was specifically associated with membranes and coenriched with synaptic vesicles when the synaptosomal fraction (P2) was further separated into the plasma membrane (LP1) and synaptic vesicle (LP2) fractions. The efficiency of the fractionation procedure was verified by detecting proteins of known localization. The synaptic vesicle membrane protein VAMP-2 was, like ICA69, greatly enriched in the LP2 fraction compared with LP1, but it was absent from the cytosolic soluble fraction S3, in which ICA69 is also abundant. In contrast, the plasma membrane marker NMDAR was enriched in LP1 and not found in the LP2 and S3 fractions. The protein SUMO-1, which in the unconjugated form detected by the antibody used here is strictly a cytosolic soluble protein (Mahajan *et al.*, 1997), was found only in the S3 fraction. Finally, the β-tubulin protein, which is cytosolic when monomeric but membrane associated in multimerized form, was found in all fractions, although it was enriched in S3.

Localization of ICA69 in the β-Cell Line HIT-1

Given that ICA69 is a diabetes autoantigen, we wished to determine the intracellular localization of ICA69 within β-cells and to determine specifically whether ICA69 colocalized with insulin granules. Western blot analysis revealed that the hamster insulinoma line HIT-1 expresses high levels of ICA69 comparable to mouse brain or pancreas (M.P., unpublished data). Immunofluorescence in HIT-1 cells to detect ICA69 and insulin revealed that both antigens are distributed in a punctate manner within the cells (Figure 2, A and B), although weak ICA69 staining was also distributed diffusely within the cytoplasm. As controls for the primary antibodies, we detected the plasma membrane marker SNAP-25 (Figure 2C), and we also used a control primary antibody (Figure 2D) that showed no nonspecific reactivity. Secondary antibodies also tested for the absence of nonspecific cross-reactivity (Figure 2, E and F) were next used in double immunofluorescence staining to determine whether ICA69 and insulin colocalize in HIT-1 cells. We found that they did not: the number of visible ICA69-positive punctate structures was fewer than the number of insulin-positive structures, and there was no colocalization between insulin staining and ICA69 staining (Figure 2, G and H). Other types of vesicles exist within β-cells, notably the SLMVs, which secrete neurotransmitters such as γ-aminobutyric acid, and it is possible that ICA69 is associated with these.

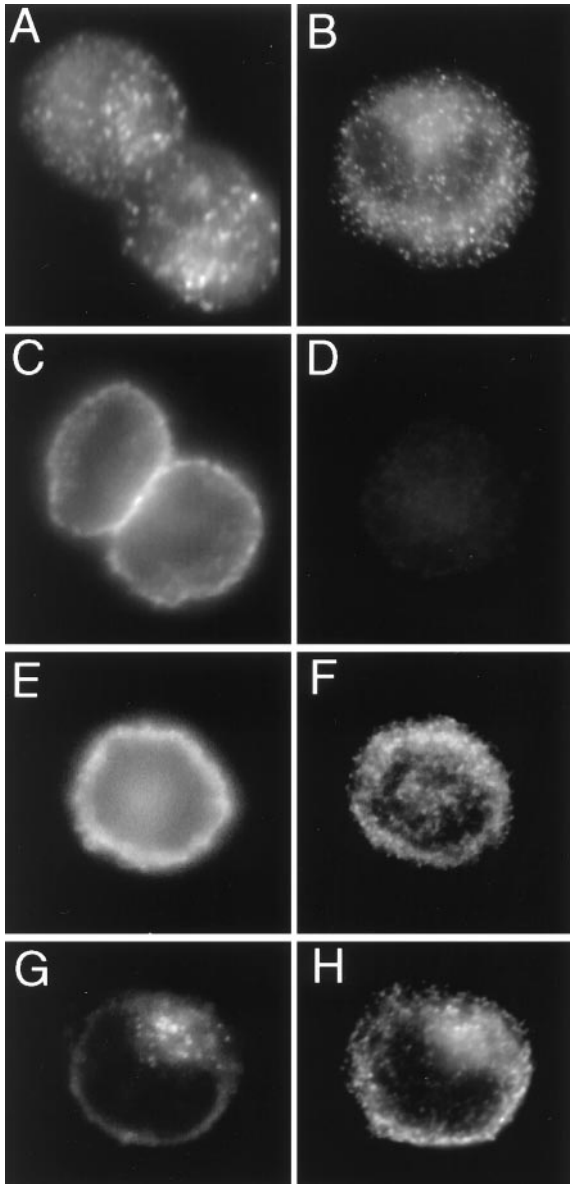

Figure 2. Immunodetection of ICA69, SNAP-25, and insulin in HIT-1 cells. (A) Two cells stained with anti-ICA69. Note the punctate distribution of the staining. (B) One cell stained with anti-insulin. Again note the punctate staining pattern. (C) Two cells stained with anti-SNAP-25. Note that the signal is localized to the plasma membrane. (D) One cell stained with a control guinea pig antibody. Note the absence of staining. (E and F) One cell costained for SNAP-25 (E) and insulin (F). Note the absence of colocalization. (G and H) One cell costained for ICA69 (G) and insulin (H). Note that although both antigens exhibit a punctate distribution, the signals do not exhibit colocalization (compare G and H).

ICA69 Homologues

Our studies of the mammalian ICA69 protein thus far suggest that it is a cytosolic protein that can associate with secretory vesicles and of which the tissue distribution correlates with secretory activity. To address more directly a possible role for ICA69 in secretory processes, we chose to exploit the model organism *C. elegans*, for which a predicted gene exists that encodes an ICA69 homologue.

Figure 3 shows the alignment of the mammalian ICA69 proteins with the predicted *Drosophila* homologue (designated CG10566 in the annotated *Drosophila* genome sequence) and the *C. elegans* homologue *ric-19* (designated C32E8.7 by the *C. elegans* Sequencing Consortium). We have confirmed the sequence and exon–intron structure of the *ric-19* cDNA between the ATG and stop codons by sequencing a reverse transcription–PCR product spanning this region. There is 15% identity among these five homologues, and an additional 17% of the amino acids are strongly similar (identical or same type of amino acids for a given position). The mammalian homologues are 87% identical to each other, and the human and *C. elegans* homologues are 33% identical overall, including a stretch of 280 amino acids exhibiting 58% conservation. The high degree of conservation between the mammalian, *Drosophila*, and *C. elegans* sequences suggests an evolutionarily conserved function. In particular, the highly conserved stretch corresponding to *ric-19* positions 141–225 may be a new functional motif. Computer analysis suggests that these proteins are cytosolic because they are hydrophilic overall and carry no signal peptides or nuclear localization signals. A coiled-coil motif may exist in the region of amino acids 175–225 of *ric-19* as well as in the corresponding regions of the mammalian and *Drosophila* homologues. Coiled coils are often implicated in protein–protein interactions, including interactions essential to vesicle trafficking and membrane fusion (Lupas, 1996; Skehel and Wiley, 1998).

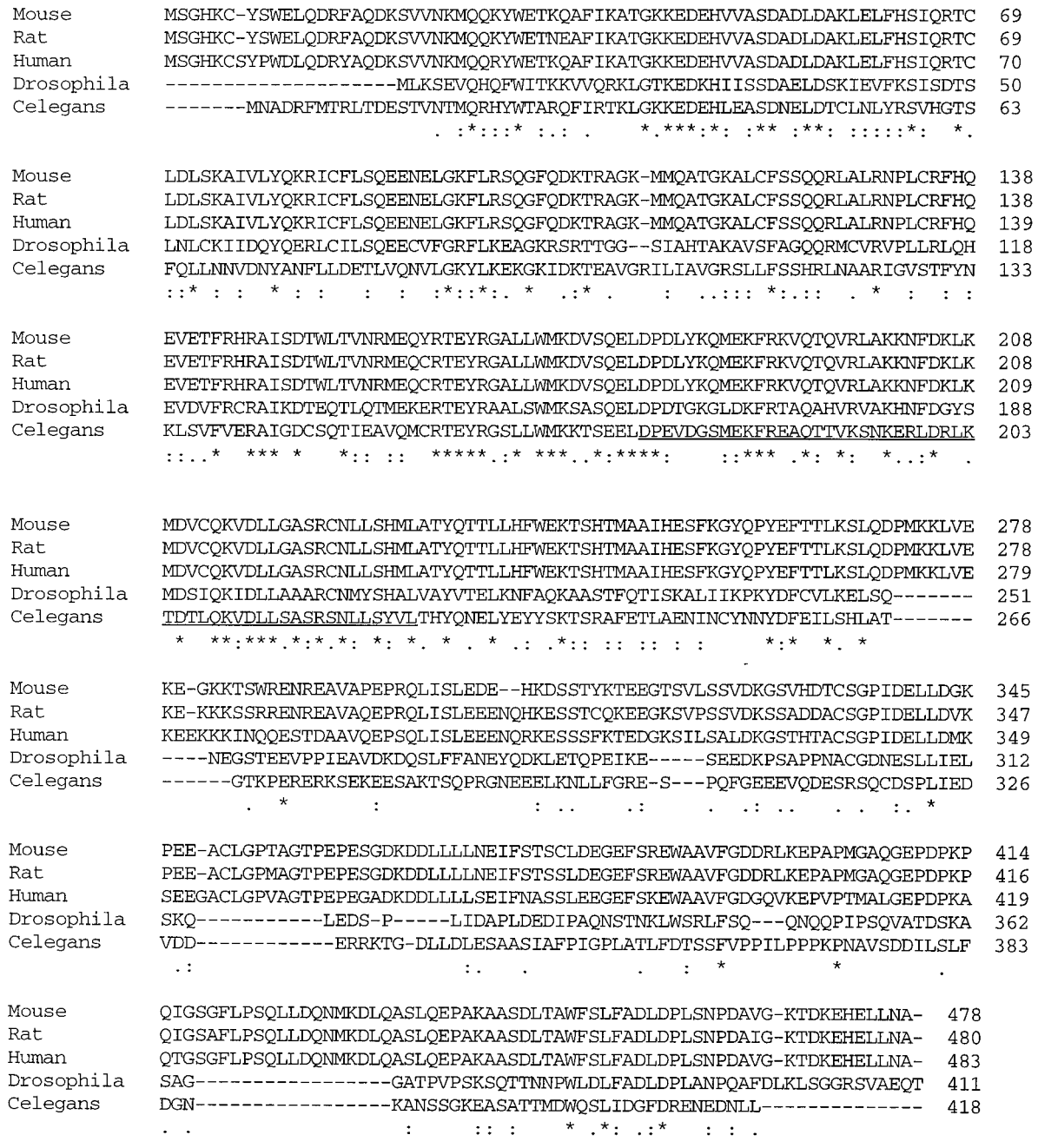

Figure 3. Alignment of the ICA69 homologues. Below the sequences, stars, colons, and periods indicate that amino acid positions are identical, highly conserved, or weakly conserved, respectively. The region predicted to encode a coiled-coil motif is underlined in the *C. elegans* sequence.

ric-19 Is Expressed in Neurons, the Canal Cell, and the Gland Cell

In an effort to ascertain the in vivo expression pattern of the *ric-19* gene, we generated transgenic lines carrying reporter genes encoding either β-galactosidase (Figure 4A) or GFP (Figure 4B) fused to a nuclear localization signal and driven by 0.6 or 1.0 kb of the *ric-19* gene. These reporter constructs all gave identical results. As shown in Figure 4, the *ric-19* promoter is active in all *C. elegans* neurons. It appeared that the *ric-19* 5′ regulatory flank is strictly neuron specific; however, because of the high expression levels in the head region of these transgenic animals (Figure 4, A and B), it was difficult to ascertain whether the secretory canal and gland cells also express the reporter genes (see below).

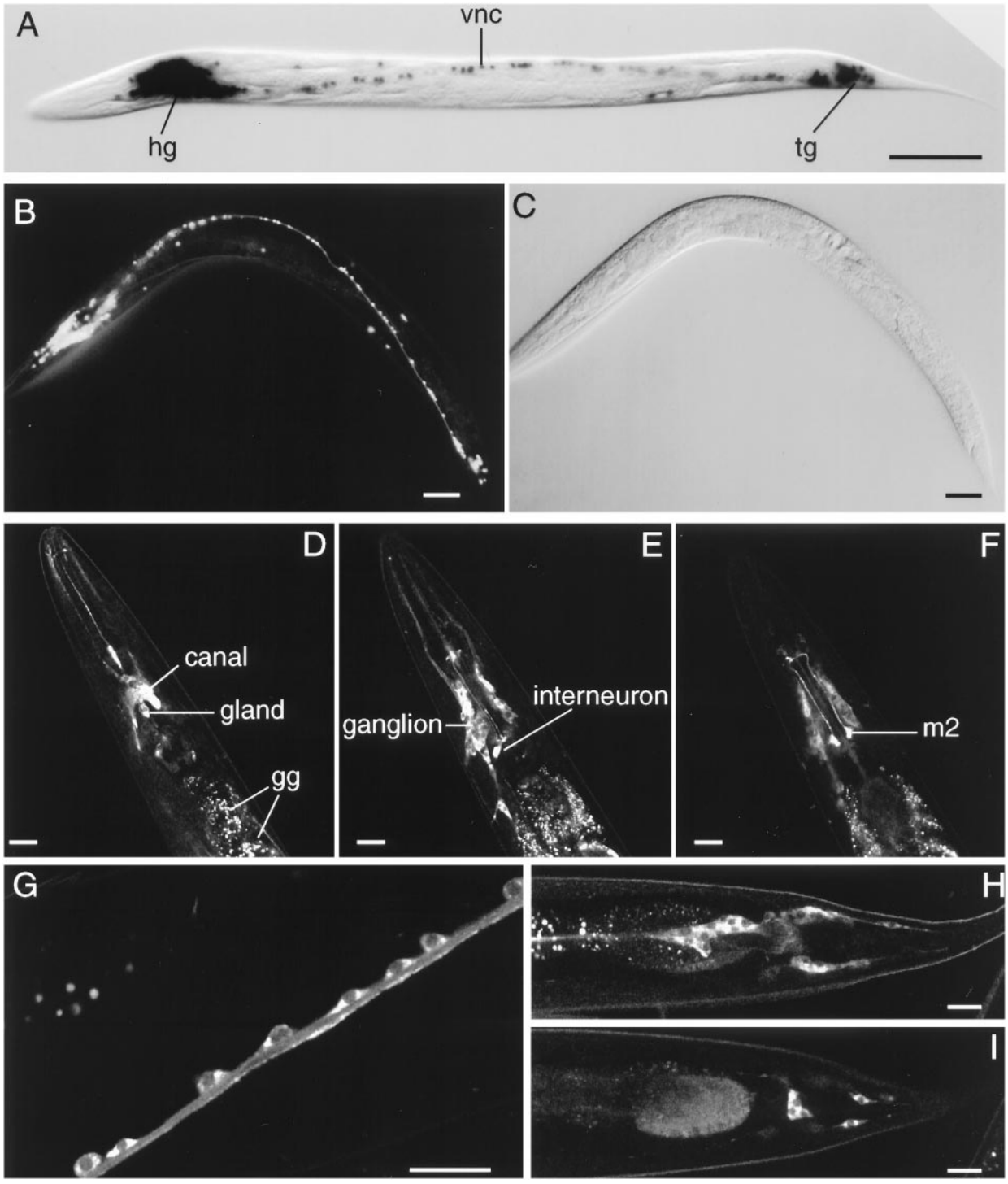

Figure 4. (A–C) In vivo *ric-19* promoter expression visualized with the use of the NLS–GFP or NLS–lacZ reporter genes. (A) NLS–lacZ staining in an animal transgenic for the array Ex[pCelicaDP-lacZ; pRF4]. (B) NLS–GFP expression in a young adult transgenic animal carrying the array Ex[pCelicaDP-GFP; pRF4]. (C) Nomarski view of panel b. hg, head ganglia; vnc, ventral nerve cord; tg, tail ganglia. Bars in A–C, 50 μm. (D–I) Confocal microscopy of transgenic animals carrying the array Ex[pRIC19::GFP; pRF4]. (D–F) Three confocal planes of the head region. In D, the excretory canal cell and gland cells are indicated; the autofluorescent gut granules (gg) are also indicated. Note the expression of the RIC-19::GFP protein in neurons of the head ganglion (most visible in E) as well as the high levels of expression in a pharyngeal interneuron (E) and m2 neurons (F). (G) A portion of the ventral nerve cord; note that the RIC-19::GFP fusion protein is expressed in the cytoplasm of each neuron shown. (H and I) Two sections of the tail region; note the expression of the RIC-19::GFP protein in the neurons of the tail ganglia. Bars in D–I, 20 μm.

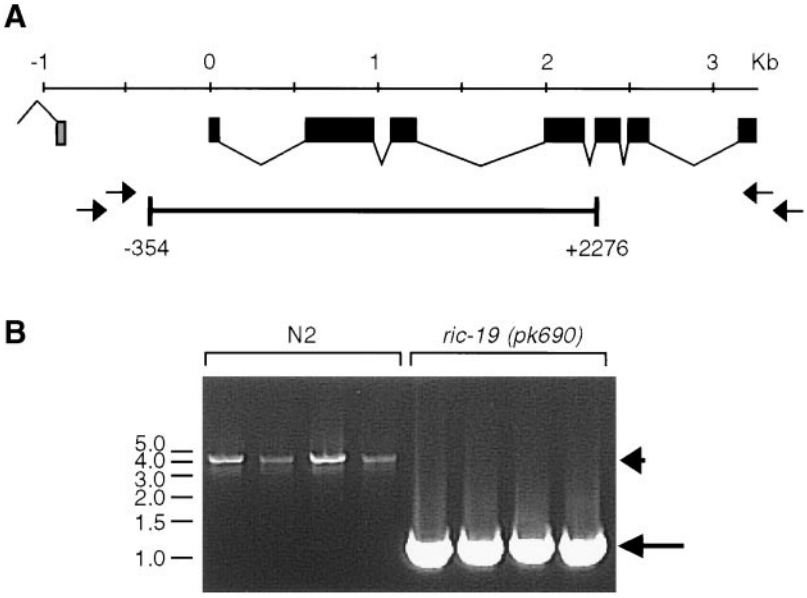

Figure 5. (A) Structure of the *ric-19* gene as well as the approximate positions of the primers used to screen and isolate a deletion mutation spanning positions −354 to 2276. (B) Example of single-worm PCR reactions with the use of the primers AR1 and AL1 on N_2 worms (lanes 1–4) or worms homozygous for the *ric-19(pk690)* allele (lanes 5–8). The arrowhead and arrow in B indicate the amplified wild-type and *pk690* alleles of *ric-19*, respectively.

To determine the expression pattern and intracellular localization of the RIC-19 protein, another set of transgenic animals was generated that carried the full-length *ric-19* gene, including 1.5 kb of 5′ flanking sequence, with the last leucine codon fused in frame with the GFP reporter and followed by the *unc-54* 3′ untranslated region. These transgenic animals expressed low levels of the RIC-19::GFP fusion protein in all neurons (Figure 4, D–I), as well as in the excretory canal and gland cells located just below the nerve ring in the head (Figure 4D). Interestingly, the m2 pharyngeal motor neurons (Figure 4F), as well as some pharyngeal interneurons (Figure 4E), expressed much higher levels of the RIC-19::GFP fusion protein than the other positive cells. The function of these neurons is not known, and their ablation does not result in any visible defect (Avery, 1993). The RIC-19::GFP protein was diffusely distributed within the cytoplasm of positive cells (Figure 4, G, H, and I).

It should be noted that the *ric-19* expression patterns reported here are tentative in that they rely on the introduction of multiple copies of reporter plasmids carried on extrachromosomal arrays in various transgenic lines. Immunostaining detection of endogenous RIC-19 protein, or in situ hybridization to visualize endogenous *ric-19* transcripts, would provide more definitive expression data.

Isolation of a ric-19 Mutant

We isolated a mutant harboring a deletion of positions −354 to +2276 of the predicted *ric-19* gene by PCR screening of a mutagenized *C. elegans* library. This deletion covers the first five of seven exons (Figure 5), thus removing the first 262 of 418 codons, including the region most conserved between the mammalian and *C. elegans* proteins. The mutant allele was designated *ric-19(pk690)* and was backcrossed 10 times onto wild-type N_2 background to produce the mutant strain AS241. Western blot analysis with the use of an antiserum directed against the terminal 20 amino acids of the RIC-19 protein detected one band of ~50 kDa in wild-type animals. This 50-kDa protein was absent in the mutant strain AS241 (Figure 6, lanes 1 and 2), suggesting that *ric-19(pk690)* is a null allele. Expression of this band was restored in transgenic mutant animals carrying the *ric-19* gene on an extrachromosomal array (Figure 6, lane 3).

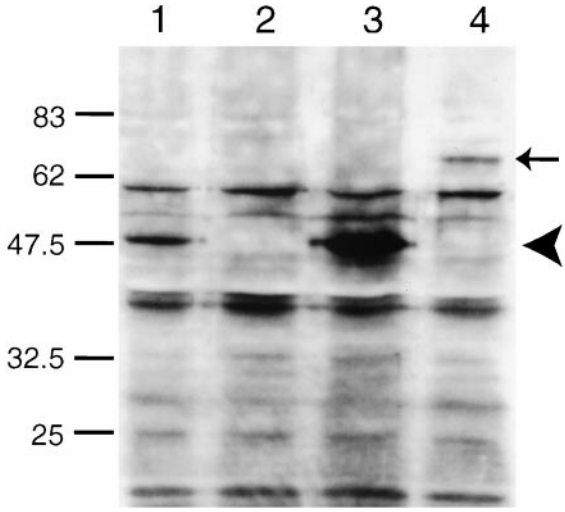

Figure 6. Western blot detection of the RIC-19 protein. Five micrograms of total worm protein was loaded in each lane and probed with a rabbit antiserum directed against a peptide corresponding to the C-terminal 20 amino acids of the RIC-19 protein. Lane 1, N_2; lane 2, AS241; lane 3, AS241 transgenic for the array Ex[pRIC-19; pRF4]; lane 4, AS241 transgenic for the array Ex[pRIC19::GFP; pRF4]. The arrowhead indicates the position of the RIC-19 protein, and the arrow indicates the position of the RIC-19::GFP fusion protein.

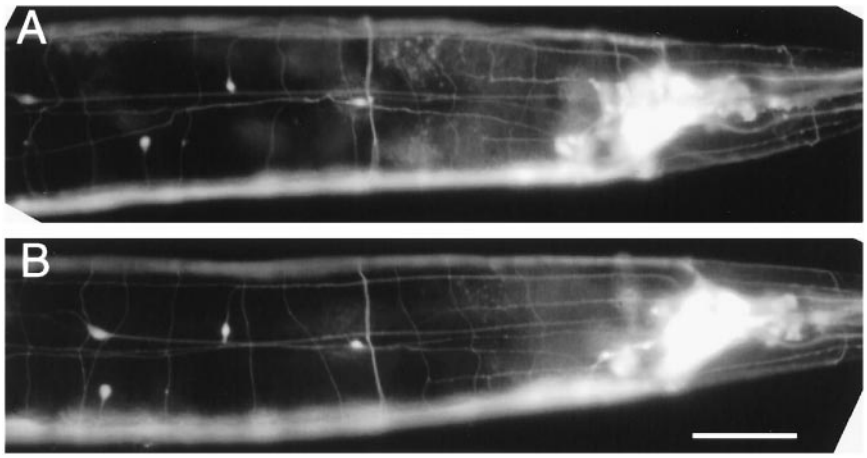

Figure 7. *ric-19(pk690)* animals exhibit no obvious abnormality in neuroarchitecture. Expression of the integrated panneuronal GFP array (*evIs11*) in wild-type (A) or *ric-19(pk690)* mutant background (B). Note that the variation in the positions of the four isolated nuclei visible in the left half of each panel is well within the norm. Bar, 20 μm.

Phenotypic Characterization of the ric-19 Mutant

Phenotypic characterization revealed that the mutant is indistinguishable from wild type in most respects, including properties that may be construed to be affected if *ric-19* was important for the function/growth of neurons, such as neuroarchitecture (Figure 7), life span, self-brood size, chemotaxis, swimming and defecation cycle length, and expulsion frequency (Table 1). The mutant also appeared normal in its ability to form males with normal mating efficiency and to form long-lived dauerlarvae upon starvation (our unpublished observations).

To investigate the possibility that *ric-19* plays a role in neurosecretory functions, we tested whether the mutant is resistant to the drugs aldicarb or levamisole. Aldicarb is an inhibitor of acetylcholinesterase and thus prevents the degradation of excess acetylcholine in the synaptic cleft, leading to paralysis. Resistance to aldicarb usually reflects a defect in neurotransmitter secretion (Miller *et al.*, 1996; Rand and Nonet, 1997). Levamisole is an agonist of acetylcholine, and resistance is usually interpreted to mean a defect in postsynaptic functions (Rand and Nonet, 1997). We found that the *ric-19* mutant is resistant to aldicarb in long-term growth rate assays (Figure 8). In particular, *ric-19(pk690)* mutant worms, but not wild-type worms, were able to proliferate in the presence of 1 mM aldicarb. No resistance to levamisole was observed (our unpublished observations). The resistance to aldicarb in the mutant suggests that *ric-19* is a novel, hitherto unknown, participant in the processes leading to and/or controlling neurotransmitter secretion.

To confirm that the aldicarb observed in the *ric-19* mutant is indeed due to disruption in the *ric-19* gene, we generated a transgenic line in which the wild-type *ric-19* gene was integrated into the genome of *ric-19(pk690)* worms. As shown in Figure 8B, the rescued animals were no longer resistant to aldicarb.

Table 1. Comparison of N_2 and *ric-19(pk690)* animals in various assays reveals no striking differences

Assay	N_2	*ric-19(pk690)*
Life span (n $\geq$ 64)	17.3 $\pm$ 0.4	17.6 $\pm$ 0.4
Brood size (n = 14)	301 $\pm$ 52	296 $\pm$ 45
Defecation interval (n = 12)	45 $\pm$ 5	44 $\pm$ 4
EMC frequency (n = 8)	100%	100%
Thrashing rate (n = 12)	121 $\pm$ 8	117 $\pm$ 8
Isobutanol C.I.	0.96	0.95
Isoamyl alcohol C.I.	0.99	0.98
Isopropanol C.I.	−0.45	−0.57
Avoidance of 4 M NaCl ring	100%	100%
T50 at 37°C (n = 12/time point)	~6 hours	~6 hours

Life span is expressed in days. Brood size is the total number of progeny per worm. Defecation interval is the number of seconds between defecations. EMC frequency is the frequency with which an expulsion muscle contraction was observed over 12 consecutive defecation cycles per worm studied. Thrashing rate is the number of trashing motions per minute. C.I. stands for Chemotaxis Index. Osmotic avoidance is given as the percentage of worms that did not cross a 4 M NaCl osmotic barrier. T50 at 37°C is the number of hours at which 50% of the test population exposed to 37°C was deemed dead. See MATERIALS AND METHODS for details and references regarding each assay.

DISCUSSION

Our results suggest that the *C. elegans* ICA69 homologue, *ric-19*, participates in neurosecretory processes. Our observation that the *ric-19* promoter is expressed strictly in neurons, the excretory canal cell, and the gland cell of *C. elegans* suggests that *ric-19* functions in specialized secretory cells. The functions of the canal and gland cells of *C. elegans* are not well characterized, but they likely include secretion of signaling molecules, such as that of a pheromone that regulates the insulin-like pathway in this organism, and of enzymes that facilitate molting (Nelson *et al.*, 1983). At the ultrastructural level, these cells exhibit features of specialized secretory cells (Nelson *et al.*, 1983). The gland cell, in particular, is rich in dense-core granules similar to the insulin secretory granules found in pancreatic β-cells (Nelson *et al.*, 1983).

Our observation that the *ric-19* deletion confers aldicarb resistance is a strong indication that the protein participates in the process of neurotransmitter secretion. *C. elegans* mu-

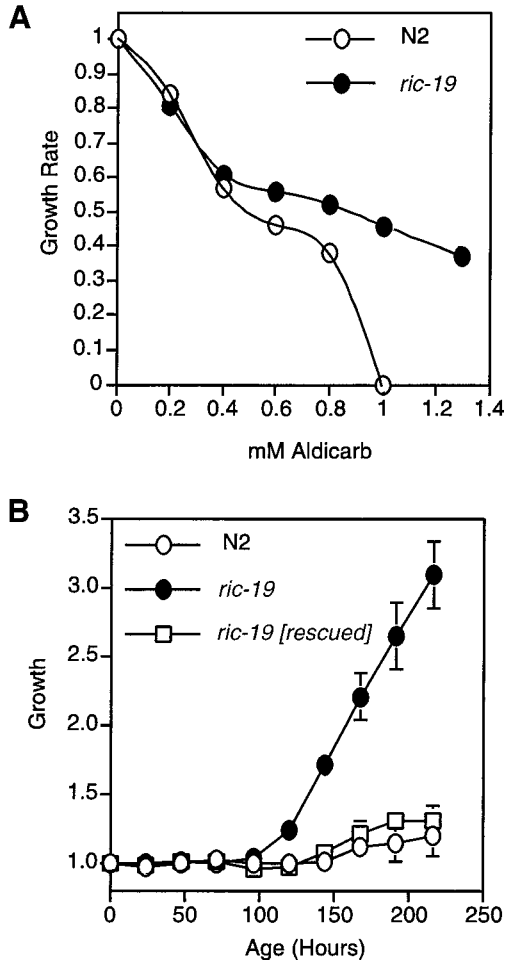

Figure 8. The *ric-19(pk690)* mutant exhibits resistance to aldicarb. (A) Relative growth rate assay. (B) Growth rate assay on NGM plates containing 1 mM aldicarb (see MATERIALS AND METHODS). *ric-19* [rescued] is a *ric-19(pk690)* mutant strain that carries an integrated array harboring the pRIC-19 expression plasmid. Error bars show the SD among five separate plates.

tations that confer resistance to inhibitors of acetylcholinesterases usually identify genes encoding components of the synaptic vesicle secretory machinery, such as RAB-3 (Nonet *et al.*, 1997), AEX-3 (Iwasaki *et al.*, 1997), synaptobrevin (Nonet *et al.*, 1998), syntaxin (Saifee *et al.*, 1998), and synaptotagmin (Nonet *et al.*, 1993). Like RIC-19, these molecules are expressed in most, if not all, *C. elegans* neurons. Synaptobrevin, a v-SNARE integral membrane protein of secretory vesicles, and syntaxin, a t-SNARE integral membrane protein present on the target membranes to which vesicles may fuse, participate in vesicle targeting, docking, and/or fusion through cognate heterotypic adhesion. RAB-3 is a small cytosolic soluble GTPase that associates with secretory vesicles when in the GTP-bound state and is thought to regulate vesicle trafficking and docking. AEX-3 is a cytosolic soluble protein that regulates RAB-3 GDP–GTP exchange. We have begun to examine possible genetic interactions between the *ric-19* mutant and other aldicarb resistance mutants. In particular, we have found that the resistance to aldicarb exhibited by the *ric-19* mutant is weaker than the resistance exhibited by the *rab-3(y250)* mutant, which is itself considered to confer relatively weak resistance (our unpublished observations). This likely explains why *ric-19* was not identified previously in screens for aldicarb resistance, which depend on rather strong resistance, and why the *ric-19* mutant exhibits no other obvious phenotype. We are currently examining possible genetic interactions between *ric-19* and other aldicarb resistance mutants by generating double mutants.

The absence of a severe phenotype in the *C. elegans ric-19* mutant suggests a regulatory or redundant, rather than essential, function for this gene. The *ric-19* gene has no other homologue in *C. elegans*, and the mammalian ICA69 gene also appears to be unique (efforts to isolate related genes by low-stringency hybridizations of mouse and human libraries have been unsuccessful; our unpublished observations). No ICA69 homologue exists within the yeast genome. An ancestral gene must have existed at a time before the separation of nematodes and mammals, some 500–700 million years ago, and this gene likely was involved in a secretory process. We are now in a position to exploit the powerful genetics of *C. elegans* to address ICA69/RIC-19 function. We can determine if a genetic interaction exists between *ric-19* and any of the other mutations described above that confer aldicarb resistance. In a more general approach, screens for enhancer mutations that confer enhanced aldicarb resistance in the *ric-19* mutant background should uncover genes that may act redundantly with *ric-19*. Furthermore, given the availability of our mutant strain made transgenic for the *ric-19* gene (Figure 7), we are now in a position to perform a screen for synthetic lethal mutations (Davies *et al.*, 1999), i.e., mutations that result in a lethal phenotype only when combined with the *ric-19* mutation.

Our reevaluation of the tissue distribution of ICA69 in the mouse shows a general correlation between secretory activity and levels of ICA69 expression (Figure 1). Subcellular fractionation of mouse brain showed that most of the ICA69 pool is present in cytosolic soluble form but that a significant portion is associated specifically with synaptic vesicles. Immunodetection of ICA69 in the hamster insulinoma line HIT-1 revealed that the protein is distributed in a punctate manner that does not correspond with insulin distribution, suggesting that in these cells ICA69 is not associated with the insulin secretory granules. ICA69 may instead associate with the SLMVs, as is the case for another diabetes autoantigen, GAD (Reetz *et al.*, 1991). Our working hypothesis is that ICA69/RIC-19 is a cytosolic soluble protein that participates in the process of vesicle secretion by interacting with the outside of vesicles, possibly via interaction with vesicle membrane proteins through coiled coils, which are present in the ICA69/RIC-19 protein.

In conclusion, several lines of evidence indicate a role for ICA69 in vesicle secretion. This is the first study aimed at dissecting ICA69 function, and our results are consistent with the interpretation that ICA69 is a cytosolic protein participating in the process of neuroendocrine secretion via association with the outside of secretory vesicles. We suggest that ICA69 should be added to the list of diabetes autoantigens that are associated with the process of regulated secretion and hope that our *ric-19 C. elegans* mutant

will prove a valuable tool in investigations of the function of this evolutionarily conserved protein.

ACKNOWLEDGMENTS

Many thanks to Karen Thijssen (The Netherlands Cancer Institute, Amsterdam, the Netherlands) for essential help in isolating the *ric-19* deletion mutant and to Prof. John White, who helped with cell identification. Some nematode strains used in this work were provided by the *Caenorhabditis* Genetics Center, which is funded by the National Institutes of Health National Center for Research Resources.

REFERENCES

Aanstoot, H.J., *et al.* (1996). Identification and characterization of glima 38, a glycosylated islet cell membrane antigen, which together with GAD65 and IA2 marks the early phases of autoimmune response in type I diabetes. J. Clin. Invest. *97*, 2772–2783.

Anderson, G.L. (1978). Responses of dauer larvae of *Caenorhabditis elegans* (Nematoda:Rhabditidae) to thermal stress and oxygen deprivation. Can. J. Zool. *56*, 1786–1791.

Avery, L. (1993). Motor neuron M3 controls pharyngeal muscle relaxation timing in *Caenorhabditis elegans*. J. Exp. Biol. *175*, 283–297.

Baekkeskov, S., Aanstoot, H., Christgau, S., Reetz, A., Solimena, M., Cascalho, M., Folli, F., Richter-Olsen, H., and De Camilli, P. (1990). Identification of the 64K autoantigen in insulin dependent diabetes as the GABA-synthesizing enzyme glutamic acid decarboxylase. Nature *347*, 151–156.

Bargmann, C.I., Harwieg, E., and Horvitz, H.R. (1993). Odorant-selective genes and neurons mediate olfaction in *C. elegans*. Cell *74*, 515–527.

Castano, L., Russo, E., Zhou, L., Lipes, M.A., and Eisenbarth, G.S. (1991). Identification and cloning of a granule autoantigen (carboxypeptidase H) associated with type I diabetes. J. Clin. Endocrinol. Metab. *73*, 1197–1201.

Chu, D.T.W., and Klymkowsky, M.W. (1989). The appearance of acetylated α-tubulin during early development and cellular differentiation. Dev. Biol. *136*, 104–117.

C. elegans Sequencing Consortium. (1998). Genome sequence of the nematode *C. elegans*: a platform for investigating biology. Science *282*, 2012–2018.

Culotti, J.G., and Russell, R.L. (1978). Osmotic avoidance defective mutants of the nematode *Caenorhabditis elegans*. Genetics *90*, 243–256.

Davies, A.G., Spike, C.A., Shaw, J.E., and Herman, R.K. (1999). Functional overlap between the mec-8 gene and five sym genes in *Caenorhabditis elegans*. Genetics *153*, 117–134.

Dotta, F., Previti, M., Neerman-Arbez, M., Dionisi, S., Cucinotta, D., Lenti, L., Di Mario, U., and Halban, P.A. (1998). The GM2-1 ganglioside islet autoantigen in insulin-dependent diabetes mellitus is expressed in secretory granules and is not beta-cell specific. Endocrinology *139*, 316–319.

Faulkner-Jones, B.E., Cram, D.S., Kun, J., and Harrison, L.C. (1993). Localization and quantitation of expression of two glutamate decarboxylase genes in pancreatic β-cells and other peripheral tissues of mouse and rat. Endocrinology *133*, 2962–2972.

Gaisano, H.Y., Sheu, L., Foskett, J.K., and Trimble, W.S. (1994). Tetanus toxin light chain cleaves a vesicle-associated membrane protein (VAMP) isoform 2 in rat pancreatic zymogen granules and inhibits enzyme secretion. J. Biol. Chem. *269*, 17062–17066.

Harlow, E., and Lane, D. (1988). Antibodies: A Laboratory Manual, Cold Spring Harbor, NY: Cold Spring Harbor Laboratory.

Hawkes, C.J., Wasmeier, C., Christie, M.R., and Hutton, J.C. (1996). Identification of the 37kDa antigen in IDDM as a tyrosine phosphatase-like protein (phogrin) related to IA-2. Diabetes *45*, 1187–1192.

Huttner, W.B., Schiebler, W., Greengard, P., and De Camilli, P. (1983). Synapsin I (protein I), a nerve terminal-specific phosphoprotein. III. Its association with synaptic vesicles studied in a highly purified synaptic vesicle preparation. J. Cell Biol. *96*, 1374–1388.

Iwasaki, K., Staunton, J., Saifee, O., Nonet, M., and Thomas, J.H. (1997). aex-3 encodes a novel regulator of presynaptic activity in *C. elegans*. Neuron *18*, 613–622.

Jansen, G., Hazendonk, E., Thijssen, K.L., and Plasterk, R.H.A. (1997). Reverse genetics by chemical mutagenesis in *Caenorhabditis elegans*. Nat. Genet. *17*, 119–121.

Karges, W., Gaedigk, R., Hui, M.F., Cheung, R., and Dosch, H.-M. (1997). Molecular cloning of murine ICA69: diabetes-prone mice recognize the human autoimmune-epitope, Tep69, conserved in splice variants from both species. Biochim. Biophys. Acta *1360*, 97–101.

Karges, W., Pietropaolo, M., Ackerley, C.A., and Dosch, H.M. (1996). Gene expression of islet cell antigen p69 in human, mouse, and rat. Diabetes *45*, 513–521.

Kenyon, C., Chang, J., Gensch, E., Rudner, A., and Tabiang, R. (1993). A *C. elegans* mutant that lives twice as long as wild type. Nature *366*, 461–464.

Lan, M.S., Lu, J., Goto, Y., and Notkins, A.L. (1994). Molecular cloning and identification of a receptor-type protein tyrosine phosphatase, IA-2, from human insulinoma. DNA Cell Biol. *13*, 505–514.

Lupas, A. (1996). Coiled coils: new structures and new functions. Trends Biochem. 375–382

Mahajan, R., Delphin, C., Guan, T., Gerace, L., and Melchior, F. (1997). A small ubiquitin-related polypeptide involved in targeting RanGAP1 to nuclear pore complex RanBP2. Cell *88*, 97–107.

Mally, M.I., Cirulli, V., Hayek, A., and Otonkoski, T. (1996). ICA69 is expressed equally in the human endocrine and exocrine pancreas. Diabetologia *39*, 474–480.

Martin, S., *et al.* (1995). Autoantibodies to the islet antigen ICA69 occur in IDDM and in rheumatoid arthritis. Diabetologia *38*, 351–355.

Mello, C., and Fire, A. (1995). DNA transformation. Methods Cell Biol. *48*, 451–482.

Mello, C.C., Kramer, J.M., Stinchcomb, D., and Ambros, V. (1991). Efficient gene transfer in *C. elegans*: extrachromosomal maintenance and integration of transforming sequences. EMBO J *10*, 3959–3970.

Miller, K.G., Alfonso, A., Nguyen, M., Crowell, J.A., Johnson, C.D., and Rand, J.B. (1996). A genetic selection for *Caenorhabditis elegans* synaptic transmission mutants. Proc. Natl. Acad. Sci. USA *93*, 12593–12598.

Miyazaki, I., Cheung, R.K., Gaedigk, R., Hui, M.F., Van der Meulen, J., Rajotte, R.V., and Dosch, H.M. (1995). T cell activation and anergy to islet cell antigen in type I diabetes. J. Immunol. *154*, 1461–1469.

Miyazaki, I., Gaedigk, R., Hui, M.F., Cheung, R.K., Morkowski, J., Rajotte, R.V., and Dosch, H.M. (1994). Cloning of human and rat p69 cDNA, a candidate autoimmune target in type I diabetes. Biochim. Biophys. Acta *1227*, 101–104.

Nelson, F.K., Albert, P.S., and Riddle, D.L. (1983). Fine structure of *Caenorhabditis elegans* secretory-excretory system. J. Ultrastruct. Res. *82*, 156–171.

Nonet, M.L., Grundahl, K., Meyer, B.J., and Rand, J.B. (1993). Synaptic function is impaired but not eliminated in *C. elegans* mutants lacking synaptotagmin. Cell *73*, 1291–1305.

Nonet, M.L., Saifee, O., Zhao, H., Rand, J.B., and Wei, L. (1998). Synaptic transmission deficits in *Caenorhabditis elegans* synaptobrevin mutants. J. Neurosci. *18*, 70–80.

Nonet, M.L., Staunton, J.E., Kilgard, M.P., Fergestad, T., Hartwieg, E., Horvitz, H.R., Jorgensen, E.M., and Meyer, B.J. (1997). *Caenorhabditis elegans* rab-3 mutant synapses exhibit impaired function and are partially depleted of vesicles. J. Neurosci. *17*, 8061–8073.

Palmer, J.P., Asplin, C.M., Clemons, P., Lyen, K., Tatpati, O., Raghu, P.K., and Paquette, T.L. (1983). Insulin antibodies in insulin-dependent diabetics before insulin treatment. Science *222*, 1337–1339.

Petersen, J.S., *et al.* (1993). Differential expression of glutamic acid decarboxylase in rat and human islets. Diabetes *42*, 484–495.

Pietropaolo, M., *et al.* (1993). Islet cell autoantigen 69 kD (ICA69): molecular cloning and characterization of a novel diabetes-associated autoantigen. J. Clin. Invest. *92*, 359–371.

Rabin, D.U., Pleasic, S.M., Shapiro, J.A., Yoo-Warren, H., Oles, J., Hicks, J.M., Goldstein, D.E., and Rae, P.M. (1994). Islet cell antigen 512 is a diabetes-specific islet autoantigen related to protein tyrosine phosphatases. J. Immunol. *152*, 3183–3188.

Rand, J.B., and Nonet, M.L. (1997). Synaptic transmission. In: *C. elegans* II, ed. D. Riddle, T. Blumenthal, B.J. Meyer, and J.R. Priess, Cold Spring Harbor, NY: Cold Spring Harbor Laboratory, 611–643.

Reetz, A., Solimena, M., Matteoli, M., Folli, F., Takei, K., and De Camilli, P. (1991). GABA and pancreatic β-cells: colocalization of glutamic acid decarboxylase (GAD) and GABA with synaptic-like microvesicles suggests their role in GABA storage and secretion. EMBO J. *10*, 1275–1284.

Riddle, D.L., Blumenthal, T., Meyer, B.J., and Priess, J.R. (eds) (1997). *C. elegans* II. Cold Spring Harbor, NY: Cold Spring Harbor Laboratory.

Roep, B.O., Arden, S.D., de Vries, R.R.P., and Hutton, J.C. (1990). T-cell clones from a type-1 diabetes patient respond to insulin secretory granule proteins. Nature *345*, 632–634.

Roep, B.O., Duinkerken, G., Schreuder, G.M.T., Kolb, H., de Vries, R.R.P., and Martin, S. (1996). HLA-associated inverse correlation between T cell and antibody responsiveness to islet autoantigen in recent-onset insulin-dependent diabetes mellitus. Eur. J. Immunol. *26*, 1285–1289.

Saifee, O., Wei, L., and Nonet, M.L. (1998). The *Caenorhabditis elegans* unc-64 locus encodes a syntaxin that interacts genetically with synaptobrevin. Mol. Biol. Cell *9*, 1235–1252.

Siegel, S.J., Brose, N., Janssen, W.G., Gasic, G.P., Jahn, R., Heinemann, S.F., and Morrison, J.H. (1994). Regional, cellular, and ultrastructural distribution of *N*-methyl-D-aspartate receptor subunit 1 in monkey hippocampus. Proc. Natl. Acad. Sci. USA *91*, 564–568.

Skehel, J.H., and Wiley, D.C. (1998). Coiled coils in both intracellular vesicle and viral membrane fusion. Cell *95*, 871–874.

Solimena, M., Dirkx, R., Hermel, J.-M., Pleasic-Williams, S., Shapiro, J.A., Caron, L., and Rabin, D.U. (1996). ICA512, an autoantigen of type I diabetes, is an intrinsic membrane protein of neurosecretory granules. EMBO J. *9*, 2102–2114.

Stassi, G., Schloot, N., and Pietropaolo, M. (1997). Islet cell autoantigen 69 kDa (ICA69) is preferentially expressed in the human islets of Langerhans than exocrine pancreas. Diabetologia *40*, 120–124.

Sulston, J.E., and Hodgkin, J.A. (1988). Methods. In: The Nematode *Caenorhabditis elegans*, ed. W.B. Wood, Cold Spring Harbor, NY: Cold Spring Harbor Laboratory, 587–606.

Thomas, J.H. (1990). Genetic analysis of defecation in *Caenorhabditis elegans*. Genetics *124*, 855–872.

Wasmeier, C., and Hutton, J.C. (1996). Molecular cloning of phogrin, a protein-tyrosine phosphatase homologue localized to insulin secretory granule membranes. J. Biol. Chem. *271*, 18161–18170.

White, J.G., Southgate, E., Thomson, J.N., and Brenner, F.R.S. (1986). The structure of the nervous system of the nematode *Caenorhabditis elegans*. Philos. Trans. R. Soc. Lond. *B314*, 1–340.

Wishart, M.J., and Dixon, J.E. (1998). Gathering STYX: phosphatase-like form predicts functions for unique protein-interaction domains. Trends Biochem. Sci. *23*, 301–306.

Wong, A., Boutis, P., and Hekimi, S. (1995). Mutations in the clk-1 gene of *Caenorhabditis elegans* affect developmental and behavioral timing. Genetics *139*, 1247–1259.

Wood, W.B. (ed.) (1988). The Nematode *Caenorhabditis elegans*. Cold Spring Harbor, NY: Cold Spring Harbor Laboratory.